PHYSICAL REVIEW D **90,** 074015 (2014)

# Spectrum of the excited $N^*$ and $\Delta^*$ baryons in a relativistic chiral quark model

E. M. Tursunov
*Institute of Nuclear Physics, Uzbekistan Academy of Sciences, 100214 Ulugbek, Tashkent, Uzbekistan*

S. Krewald
*Institute fuer Kernhysik, Forschungszentrum Juelich, 52425 Juelich, Germany*

(Received 18 April 2012; revised manuscript received 1 August 2014; published 10 October 2014)

The spectrum of the SU(2) flavor baryons is studied in the frame of a relativistic chiral quark potential model based on the one-pion and one-gluon exchange mechanisms. It is argued that the $N^*$ and $\Delta^*$ resonances strongly coupled to the $\pi N$ channel are identified with the orbital configurations $(1S_{1/2})^2(nlj)$ with a single valence quark in the excited state $(nlj)$. With the obtained selection rules based on the "chiral constraint," we show that it is possible to construct a schematic periodic table of baryon resonances, consistent with the experimental data and yielding no "missing resonances." A new original method for the treatment of the center of mass problem is suggested which is based on the separation of the three-quark Dirac Hamiltonian into the parts, corresponding to the Jacobi coordinates. The numerical estimations for the energy positions of the nucleon and delta baryons (up to and including F-wave $N^*$ and $\Delta^*$ resonances), obtained within the field-theoretical framework by using time ordered perturbation theory, yield an overall good description of the experimental data at the level of the relativized constituent quark model of S. Capstick and W. Roberts without any fitting parameters. The only free parameter of the linear confinement potential was fitted previously by Th. Gutsche to reproduce the axial charge of the nucleon. The ground state $\Delta(1232)$ is well reproduced. However, nucleon ground state and most of the radially excited baryon resonances (including Roper) are overestimated. On the contrary, the first band of the orbitally excited baryon resonances with a negative parity are underestimated. At the same time, the second band of the orbitally excited $\Delta^*$ states with the negative parity are mostly overestimated, while the $N^*$ states are close to the experimental boxes. The theoretical estimations of the energy levels for the positive parity baryon resonances with $J = 5/2, 7/2$ are close to the experimental data. At higher energies, where the experimental data are poor, we can extend our model schematically and predict an existence of seven $N^*$ and four $\Delta^*$ new states with larger spin values.

DOI: 10.1103/PhysRevD.90.074015 PACS numbers: 12.39.Fe, 11.10.Ef, 12.39.Ki, 12.40.Yx

## I. INTRODUCTION

Presently, several experimental collaborations study the production and decay of excited baryons motivated by open questions concerning the origin of the hadronic masses [1]. The successes of lattice quantum chromodynamics(QCD) in describing the ground state hadrons confirm the QCD Lagrangian in the nonperturbative regime of the strong interaction [2]. First studies of the masses of excited baryons are available [3–5]. While the lattice simulations are numerically very involved, there are simpler empirical rules which work amazingly well: the Forkel-Klempt mass formula reproduces the known $N^*$ and $\Delta^*$ masses with three parameters [1]. The question arises whether the lattice results can be interpreted by simpler models, such as flux tubes or constituent quarks. The constitutent quark models (CQM) are the oldest approaches to baryon spectroscopy and have evolved into three major subspecies, based on the Goldstone-boson exchange (GBE) [6], the one-gluon exchange (OGE) [7,8] or (and) instanton induced exchange (IIE) [9] mechanisms between (non)relativistic constituent quarks. In the present approach, we start from relativistic chiral quark models [10–15] which respect the chiral symmetry. There are no studies of the excited baryon spectrum within these approaches in the literature.

In [16–18] we have developed a relativistic chiral quark model for the lower excitation spectrum of the nucleon and delta. The splitting of the Roper resonance from the N(939) was reproduced with a reasonable accuracy. The model was tested first in Ref. [19] for the study of the nucleon charge form factors, then in Refs. [20,21] for the study of the nucleon properties such as mass, charge radius, magnetic moment, axial charge, and reasonable agreement with the experimental values was obtained. A slightly modified version of the model was extensively used for the study of the ground state baryon properties, such as masses and electromagnetic structure in Refs. [22–27], and for the detailed analysis of the meson-nucleon sigma terms in Refs. [28,29], and also for the study of the strange nucleon form factors in Ref. [30].

The model is based on an effective chiral Lagrangian. Quark wave function is obtained from the solution of the

 

Dirac equation with a Cornell type potential containing a linear confining term and a Coulomb part due to short range gluon field correlations. All the model parameters of the model, except one are fixed from the Lattice study of previous authors [31,32]. The only free parameter of the model is the so-called "mass term" in the confinement potential, which was fitted in Ref. [21] to reproduce the axial charge of the nucleon. The calculations are done at one loop or at order of accuracy $o(1/f_\pi^2, \alpha_s)$.

The aim of the present paper is to extend the relativistic chiral quark model to the higher excitation spectrum of SU(2) flavor baryons. First we want to check, whether the relativistic chiral quark model can help to understand the systematics of the excited nucleon and delta states and an orbital structure of each baryon state. Based on selection rules obtained from one-pion exchange mechanisms between valence quarks, below we will show that it is possible to construct a periodic table, where each excited Nucleon or Delta state can be identified with an orbital configuration $(1S)^2(nlj)$ with a single radially or/and orbitally excited valence quark.

Second we will estimate the excited nucleon and delta spectrum in the present model with taking into account second-order perturbative corrections due to the pion and color-magnetic gluon fields and compare with the experimental data.

The relevant suggestion is that the results of our study can be reproduced in any chiral quark model describing the baryons as bound states of three valence quarks with a Dirac two-component structure and surrounded by the cloud of $\pi$-mesons, as required by the chiral symmetry [33].

In Sec. II we give the main formalism of the model. The numerical results are presented in Sec. III, and final conclusions are given in Sec. IV.

## II. MODEL

### A. Basis formalism

The effective Lagrangian of the model $\mathcal{L}(x)$ (see [20,34]) contains the quark core part $\mathcal{L}_Q(x)$, the quark-pion $\mathcal{L}_I^{(q\pi)}(x)$ and the quark-gluon $\mathcal{L}_I^{(qg)}(x)$ interaction terms, and the kinetic parts for the pion $\mathcal{L}_\pi(x)$ and gluon $\mathcal{L}_g(x)$ fields:

$$\begin{aligned}\mathcal{L}(x) &= \mathcal{L}_Q(x) + \mathcal{L}_I^{(q\pi)}(x) + \mathcal{L}_I^{(qg)}(x) + \mathcal{L}_\pi(x) + \mathcal{L}_g(x)\\ &= \bar\psi(x)[i\partial - S(r) - \gamma^0 V(r)]\psi(x)\\ &\quad - 1/f_\pi \bar\psi[S(r) i\gamma^5 \tau^i \phi_i]\psi - g_s \bar\psi A_\mu^a \gamma^\mu \frac{\lambda^a}{2}\psi\\ &\quad + \frac{1}{2}(\partial_\mu \phi_i)^2 - \frac{1}{2} m_\pi^2 \phi_i^2 - \frac{1}{4} G_{\mu\nu}^a G_a^{\mu\nu}. \end{aligned} \quad (1)$$

Here, $\psi(x)$, $\phi_i$, $i = 1, 2, 3$ and $A_\mu^a$ are the quark, pion, and gluon fields, respectively. The matrices $\tau^i$ $(i = 1, 2, 3)$ and $\lambda^a$ $(a = 1, \ldots, 8)$ are the isospin and color matrices, correspondingly. The pion decay constant $f_\pi = 93$ MeV. In the model, the chiral symmetry violated through the quark confinement mechanism is restored with the help of the linearized $\sigma$-model. The mass term for the pion field is introduced in order to satisfy the PCAC theorem [35], which is consistent with the Goldberger-Treiman relation.

We use the Cornell type potential in the Dirac equation for the single quark states in accordance with the lattice QCD theory. The scalar part of the static confinement potential is given by

$$S(r) = cr + m, \quad (2)$$

where $c$ and $m$ are constants. The strength parameter $c$ of the confinement potential is defined from the lattice study [31], while $m$ is the only free parameter of the model which can be fitted to reproduce the axial charge $g_A$ of the proton (and the $\pi NN$ coupling constant via the Goldberger-Treiman relation).

At short distances, transverse fluctuations of the string are dominating [36], with an indication that they transform like the time component of the Lorentz vector. They are given by a Coulomb type vector potential (the so-called Luscher term) as

$$V(r) = -\alpha/r, \quad (3)$$

where $\alpha = \pi/12$ is defined from the QCD lattice study [32].

The quark fields are obtained from solving the Dirac equation with the corresponding scalar plus vector potentials

$$[i\gamma^\mu \partial_\mu - S(r) - \gamma^0 V(r)]\psi(x) = 0. \quad (4)$$

The respective positive and negative energy eigenstates as solutions to the Dirac equation with a spherically symmetric mean field, are given in a general form as

$$u_\alpha(x) = \begin{pmatrix} g_{N\kappa}^+(r) \\ -if_{N\kappa}^+(r)\vec\sigma\,\hat{\vec x}\end{pmatrix} \mathcal{Y}_\kappa^{m_j}(\hat{\vec x})\chi_{m_t}\chi_{m_c}\exp(-iE_\alpha t), \quad (5)$$

$$v_\beta(x) = \begin{pmatrix} g_{N\kappa}^-(r) \\ -if_{N\kappa}^-(r)\vec\sigma\,\hat{\vec x}\end{pmatrix} \mathcal{Y}_\kappa^{m_j}(\hat{\vec x})\chi_{m_t}\chi_{m_c}\exp(+iE_\beta t). \quad (6)$$

The quark and antiquark eigenstates $u$ and $v$ are labeled by the radial, angular, azimuthal, isospin, and color quantum numbers $N$, $\kappa$, $m_j$, $m_t$, and $m_c$, which are collectively denoted by $\alpha$ and $\beta$, respectively. The spin-angular part of the quark field operators

$$\mathcal{Y}_\kappa^{m_j}(\hat{\vec x}) = [Y_l(\hat{\vec x}) \otimes \chi_{1/2}]_{jm_j} j = |\kappa| - 1/2. \quad (7)$$

The quark fields $\psi$ are expanded over the basis of positive and negative energy eigenstates as

$$\psi(x) = \sum_\alpha u_\alpha(x) b_\alpha + \sum_\beta v_\beta(x) d^\dagger_\beta. \tag{8}$$

The expansion coefficients $b_\alpha$ and $d^\dagger_\beta$ are operators, which annihilate a quark and create an antiquark in the orbits $\alpha$ and $\beta$, respectively.

The free pion field operator is expanded over plane wave solutions as

$$\phi_j(x) = (2\pi)^{-3/2} \int \frac{d^3k}{(2\omega_k)^{1/2}} [a_{j\mathbf{k}} \exp(-ikx) + a^\dagger_{j\mathbf{k}} \exp(ikx)] \tag{9}$$

with the usual destruction and creation operators $a_{j\mathbf{k}}$ and $a^\dagger_{j\mathbf{k}}$, respectively. The pion energy is defined as $\omega_k = \sqrt{k^2 + m_\pi^2}$. The free gluon field operators is expanded in the same way.

In denoting the three-quark vacuum state by $|0\rangle$, the corresponding noninteracting many-body quark Green's function (propagator) of the quark field is given by the customary vacuum Feynman propagator for a binding potential [37]:

$$\begin{aligned} iG(x,x') &= iG^F(x,x') = \langle 0|T\{\psi(x)\bar\psi(x')\}|0\rangle \\ &= \sum_\alpha u_\alpha(x)\bar u_\alpha(x')\theta(t-t') \\ &\quad + \sum_\beta v_\beta(x)\bar v_\beta(x')\theta(t'-t). \end{aligned} \tag{10}$$

Since the three-quark vacuum state $|0\rangle$ does not contain any pion or gluon, the pion and gluon Green's functions are given by the usual free Feynman propagator for a boson field:

$$\begin{aligned} i\Delta_{ij}(x-x') &= \langle 0|T\{\phi_i(x)\bar\phi_j(x')\}|0\rangle \\ &= i\delta_{ij} \int \frac{d^4k}{(2\pi)^4} \frac{1}{k^2 - m_\pi^2 + i\epsilon} \exp[-ik(x-x')], \end{aligned} \tag{11}$$

$$\begin{aligned} i\Delta^{(\mu\nu)}_{ab}(x-x') &= \langle 0|T\{A^a_\mu(x)A^b_\nu(x')\}|0\rangle \\ &= i\delta_{ab} g^{\mu\nu} \int \frac{d^4k}{(2\pi)^4} \frac{1}{k^2 + i\epsilon} \exp[-ik(x-x')], \end{aligned} \tag{12}$$

(in the Coulomb gauge), where $g^{\mu\nu} = \delta_{\mu\nu} g^{\mu\mu}$, $g^{00} = -g^{11} = -g^{22} = -g^{33} = 1$.

In Ref. [23] the authors have shown that the initial effective Lagrangian Eq. (1) of the chiral quark model and the renormalized Lagrangian which includes counterterms yield the same expression for the mass spectrum of the nucleon. Assuming that this is true for all SU(2) baryons, we use the initial effective Lagrangian as the basis for the estimations of the ground and excited baryon mass spectra.

On the basis of the effective Lagrangian and using the time-ordered perturbation theory within the frame of many-body quantum field theory [37] we can develop the calculation scheme for the excitation spectrum of the nucleon and delta.

At zeroth order the quark core result ($E_Q$) is obtained by solving Eq. (4) for the single quark system numerically by using the harmonic oscillator basis. Since we work in the independent particle model, we assume that the bare three-quark state of the $SU(2)$-flavor baryons corresponds to the structure $(1S_{1/2})^2(nlj)$ with a single excited valence quark in the nonrelativistic spectroscopic notation. Below, on the basis of the one-pion and one-gluon exchange mechanisms we will argue that such a configuration of the three valence quarks is identified with the baryon resonances decaying strongly into the $\pi + N$ channel. And to the contrary, the baryon states with more than one valence quarks in excited orbits do not have a strong coupling into this channel. In other words, all baryon resonances appearing in the $\pi N$ scattering data can be identified with the above orbital configuration containing a single excited valence quark. This is why we fix the excited baryon configuration as $(1S_{1/2})^2(nlj)$. The corresponding quark core energy is evaluated as the sum of single quark energies with:

$$E_Q = 2E(1S_{1/2}) + E(nlj). \tag{13}$$

The second order perturbative corrections to the energy spectrum of the SU(2) baryons due to the pion ($\Delta E^{(\pi)}$) and gluon ($\Delta E^{(g)}$) fields are calculated on the basis of the Gell-Mann and Low theorem:

$$\begin{aligned} \Delta E = \Bigg\langle \Phi_0 \Big| \sum_{n=1}^{\infty} \frac{(-i)^n}{n!} \int i\delta(t_1) d^4x_1 \ldots d^4x_n T \\ \times [\mathcal{H}_I(x_1)\ldots\mathcal{H}_I(x_n)] \Big| \Phi_0 \Bigg\rangle_c \end{aligned} \tag{14}$$

with $n = 2$, where the relevant quark-pion and quark-gluon interaction Hamiltonian densities are

$$\mathcal{H}^{(q\pi)}_I(x) = \frac{i}{f_\pi} \bar\psi(x)\gamma^5 \vec\tau \vec\phi(x) S(r) \psi(x), \tag{15}$$

$$\mathcal{H}^{(qg)}_I(x) = g_s \bar\psi(x) A^a_\mu(x) \gamma^\mu \frac{\lambda^a}{2} \psi(x). \tag{16}$$

The stationary bare three-quark state $|\Phi_0\rangle$ is constructed from the vacuum state using the usual creation operators:

$$|\Phi_0\rangle_{\alpha\beta\gamma} = b^+_\alpha b^+_\beta b^+_\gamma |0\rangle, \tag{17}$$

where $\alpha$, $\beta$, and $\gamma$ represent the quantum numbers of the single quark states, which are coupled to the respective

baryon configuration. The energy shift of Eq. (14) is evaluated up to second order in the quark-pion and quark-gluon interaction, and generates self-energy and exchange diagrams contributions. In the self-energy diagrams a single pion or gluon is emitted and absorbed by the same valence quark, which however can be excited to an intermediate quark or antiquark state. In the second order exchange diagrams a single pion or gluon, emitted by a valence quark is absorbed by another valence quark of the SU(2) baryon.

### B. Center of mass corrections for the ground state N and Δ

The result for $E_Q$ in Eq. (13) contains an essential spurious contribution of the center of mass motion to the energy of the baryons. A covariant way of the separation of the CM motion is possible in nonrelativistic models. In the nonrelativistic three nucleon system the energy is reduced by factor about $1/3$ after the separation of the CM. At the same time different approaches are being used in relativistic mean field models.

For the ground state nucleon and delta baryons we use the development of the Ref. [38], where three different approximations have been used, which estimate corrections for the center of mass motion: the $R = 0$ [39], $P = 0$ [40], and LHO [41] methods. In all three methods the baryon wave function is rewritten in the Jacobi coordinates in the center of mass system as $\Phi_B(\vec{r}, \vec{\rho}, \vec{R})$, where $\vec{r}$, $\vec{\rho}$, and $\vec{R}$ are relative coordinates between the two valence quarks, between 3-valence quark and the center of mass of the $1 + 2$ quarks, and the center of mass of the all three quarks, respectively:

$$\begin{aligned}\vec{r} &= \vec{r}_1 - \vec{r}_2,\\ \vec{\rho} &= (\vec{r}_1 + \vec{r}_2)/2 - \vec{r}_3,\\ \vec{R} &= (\vec{r}_1 + \vec{r}_2 + \vec{r}_3)/3.\end{aligned} \tag{18}$$

The initial baryon wave function $\Phi(\vec{r}_1, \vec{r}_2, \vec{r}_3)$ expanded in the oscillator basis states are transformed to the Jacobi coordinates by using the Moshinsky transformation (see Ref. [38] for details).

In the R = 0 method the baryon wave function in the CM system is multiplied by the plane wave of the CM motion:

$$\Phi_R(\vec{r}_1, \vec{r}_2, \vec{r}_3, \vec{P}) = N_R \exp(i\vec{P}\cdot\vec{R})\Phi_B(\vec{r}, \vec{\rho}, \vec{R} = 0). \tag{19}$$

The second P = 0 method is based on the Fourier transformation of the baryon wave function:

$$\Phi_P(\vec{r}_1, \vec{r}_2, \vec{r}_3, \vec{P}) = N_P \exp(i\vec{P}\cdot\vec{R}) \times \int \exp(-i\vec{P}\cdot\vec{R}')\Phi_B(\vec{r}, \vec{\rho}, \vec{R}')d\vec{R}'. \tag{20}$$

The lowest harmonic oscillator (LHO) method is based on the projection of the baryon wave function on the lowest harmonic oscillator state:

$$\Phi_{\rm LHO}(\vec{r}_1, \vec{r}_2, \vec{r}_3, \vec{P}) = N_{\rm LHO}\exp(i\vec{P}\cdot\vec{R}) \times \int R_{0s}(\vec{R}')\Phi_B(\vec{r}, \vec{\rho}, \vec{R}')d\vec{R}'. \tag{21}$$

The factors $N_R$, $N_P$, and $N_{\rm LHO}$ differ each from other and are found from the normalization conditions:

$$\langle\Phi(\vec{r}_1, \vec{r}_2, \vec{r}_3, \vec{P})|\Phi(\vec{r}_1, \vec{r}_2, \vec{r}_3, \vec{P}')\rangle = (2\pi)^3\delta(\vec{P} - \vec{P}'). \tag{22}$$

In all of the three methods, the average kinetic energy and mass terms of the three-body system are estimated by using angular momentum algebra and numerical methods (see Ref. [38] for details).

### C. Center of mass corrections for the excited states N* and Δ*

For the excited nucleon and delta states with fixed orbital configuration $(1S)^2(nlj)$, the Moshinsky transformation is not applicable due to two-component structure of the valence quark wave functions. An original new approach to the center of mass correction problem is based on the separation of the total three-quark core Dirac Hamiltonian with the scalar and vector mean field potentials

$$\hat{H} = \sum_{i=1}^{3}[\vec{\alpha}_i\,\vec{p}_i + S(\vec{r}_i - \vec{R})\beta_i + V(\vec{r}_i - \vec{R})] \tag{23}$$

into two parts corresponding to the relative motion and center of mass motion, respectively. In this way one can estimate the zero-order quark-core energy for the baryon states with fixed orbital configurations $(1S)^2(nlj)$ free off the center of mass motion by solving the corresponding equation. At the zero order the energy values of all baryon states with fixed orbital configuration degenerate. This means that one can estimate the zero-order energy values of baryon states with the fixed orbital configuration $(1S)^2(nlj)$, assuming that the two S-quarks are in the $^1S_0$ singlet scalar diquark state.

The kinetic energy term can be rewritten easily as:

$$\begin{aligned}\hat{H}_0 &= \hat{H}_{R,0} + \hat{H}_{\rm rel,0},\\ \hat{H}_{R,0} &= \frac{\vec{\alpha}_1 + \vec{\alpha}_2 + \vec{\alpha}_3}{3}\vec{P}_R,\\ \hat{H}_{\rm rel,0} &= (\vec{\alpha}_1 - \vec{\alpha}_2)\vec{P}_r + \left(\frac{\vec{\alpha}_1 + \vec{\alpha}_2}{2} - \vec{\alpha}_3\right)\vec{P}_\rho.\end{aligned} \tag{24}$$

First we study the center of mass motion problem for the scalar-vector mean-field potential of the oscillator form

$$\hat{H}_{\rm int} = \sum_{i=1}^{3}[V_1(\vec{r}_i - \vec{R})\beta_i + V_2(\vec{r}_i - \vec{R})],$$
$$V_k(\vec{r}_i) = c_k r_i^2 + \mu_k, \quad k = 1, 2. \tag{25}$$

In this case the interaction part of the three-quark core Hamiltonian can be exactly separated in Jacobi coordinates as

$$\hat{H}_{\rm int} = V_r + V_\rho,$$
$$V_r = 1/2(c_1\beta_r + c_2)r^2 + 2(\mu_1\beta_r + \mu_2),$$
$$V_\rho = 2/3(c_1\beta_\rho + c_2)\rho^2 + \mu_1\beta_\rho + \mu_2, \tag{26}$$

where we introduced the Dirac matrices $\beta_r$ and $\beta_\rho$ corresponding to the Jacobi coordinates $r$ and $\rho$, respectively. In consistency with the above assumption, that the two S-quarks are in the singlet $^1S_0$ state and combining the kinetic and interaction parts of the relative motion Hamiltonian for the case of the oscillator scalar-vector mean field potentials we can write down:

$$\hat{H}_{\rm rel} = \hat{H}_r + \hat{H}_\rho, \tag{27}$$

where the Hamiltonian $\hat{H}_r$ corresponds to the singlet diquark relative motion, and the Hamiltonian $\hat{H}_\rho$ is related to the single excited valence quark motion with the modified potentials:

$$\hat{H}_r = (\vec{\alpha}_1 - \vec{\alpha}_2)\vec{P}_r + V_r$$
$$\hat{H}_\rho = -\vec{\alpha}_3\vec{P}_\rho + V_\rho. \tag{28}$$

The two-body Dirac equation

$$\hat{H}_r\Psi(\vec{r}) = E_r\Psi(\vec{r}) \tag{29}$$

can be solved in the same way as the single particle Dirac equation with the only difference that the lower component of the two-body Dirac wave function differs from the upper component by the both spin and orbital momentum. This result is a consequence of the relation:

$$(\vec{\sigma}_1 - \vec{\sigma}_2)\hat{\vec{r}}\mathcal{Y}^{jm_j}_{l,S}(\hat{\vec{r}}) = -2\sqrt{3}\sum_h (2h+1)\begin{Bmatrix} \frac{1}{2} & \frac{1}{2} & S \\ l & j & h \end{Bmatrix} \times \begin{Bmatrix} \frac{1}{2} & \frac{1}{2} & (S\pm 1) \\ (l\pm 1) & j & h \end{Bmatrix} \times \mathcal{Y}^{jm_j}_{l\pm 1,S\pm 1}(\hat{\vec{r}}), \tag{30}$$

where

$$\mathcal{Y}^{jm_j}_{lS}(\hat{\vec{r}}) = [Y_l(\hat{\vec{r}}) \otimes \chi_S(1,2)]_{jm_j}, \tag{31}$$

which shows us the correct form for the two-body Dirac bound state wave function to be as

$$\Psi(\vec{r}) = \begin{pmatrix} g_{N,l}(r)\mathcal{Y}^{jm_j}_{l,S}(\hat{\vec{r}}) \\ if_{N,l\pm 1}(r)\mathcal{Y}^{jm_j}_{l\pm 1,S\pm 1}(\hat{\vec{r}}) \end{pmatrix}. \tag{32}$$

The radial wave functions $g_{N,l}(r)$ and $f_{N,l}(r)$ are expanded over the oscillator basis states as was done for the single quark wave function. For the scalar diquark in the ground state the upper and lower components of the two-body Dirac wave function present the $^1S_0$ and $^3P_0$ waves, respectively. The estimated energy value of the Eq. (29) together with the solution of the single-quark Dirac equation

$$\hat{H}_\rho\Psi(\vec{\rho}) = E_\rho\Psi(\vec{\rho}) \tag{33}$$

with the modified potential Eq. (26) yield us the quark core results of the energy value for the excited baryon states with the fixed orbital configuration $(1S)^2(nlj)$

$$E_0 = E_r + E_\rho \tag{34}$$

free off the center of mass contribution. Thus, we found a way to separate the center of mass motion of the three-quark system bound by the scalar-vector mean-field oscillator potentials.

Now we return to the Eq. (23) with the interaction Hamiltonian

$$\hat{H}_{\rm int} = \sum_{i=1}^{3}[S(\vec{r}_i - \vec{R})\beta_i + V(\vec{r}_i - \vec{R})], \tag{35}$$

with the linear scalar $S(r) = cr + m$ [see Eq. (2)] and Coulomb-like vector $V(r) = -\alpha/r$ [see Eq. (3)] mean-field potentials. For these potentials, unlike scalar-vector mean-field potentials, the separation of the interaction Hamiltonian on the potentials $V_r$ and $V_\rho$, dependent on the Jacobi coordinates $r$ and $\rho$, respectively, is a strong task. For the confinement potential in the Jacobi coordinates we have an expansion over multipoles

$$\hat{S}(\vec{r},\vec{\rho}) = \sum_{i=1}^{3} S(\vec{r}_i - \vec{R}) = 2c\sum_{l=0,2,\ldots}\frac{(\rho/3)^l}{(r/2)^{l+1}}\left[\frac{\rho^2/9}{2l+3} - \frac{r^2/4}{2l-1}\right]P_l(\cos(\hat{\vec{r}},\hat{\vec{\rho}})) + \frac{2}{3}c\rho + 3m, \tag{36}$$

where $P_l(\cos(\hat{\vec{r}},\hat{\vec{\rho}}))$ are the Legandre polynomials. The Coulomb-like potential is transformed in the same way into the Jacobi coordinates as

$$\hat{V}(\vec{r},\vec{\rho}) = \sum_{i=1}^{3} V(\vec{r}_i - \vec{R}) = -\frac{4\alpha}{r}\sum_{l=0,2,\ldots}\left(\frac{\rho/3}{r/2}\right)^l P_l(\cos(\hat{\vec{r}},\hat{\vec{\rho}})) - \frac{3\alpha}{2\rho}. \tag{37}$$

The above equations are valid for $\rho/3 < r/2$. In the rest area these variables must be interchanged. Thus, in the Jacobi coordinates we come to the situation, when the original linear confinement and Coulomb-like potentials depend on the angle between the Jacobi coordinate-vectors $\vec{r}$ and $\vec{\rho}$. However, at first approximation when keeping the main multipoles, these potentials can be written as

$$\hat{S}(\vec{r},\vec{\rho}) \approx cr + \frac{2}{3}c\rho + 3m,$$
$$\hat{V}(\vec{r},\vec{\rho}) \approx -\frac{4\alpha}{r} - \frac{3\alpha}{2\rho}. \quad (38)$$

On the basis of the last approximation we divide the confinement and Coulomb potential terms in the Jacobi coordinates into two parts according to the Eq. (28) and corresponding to the scalar diquark plus the modified single quark Hamiltonians. The first test calculations can be done for the separation

$$\hat{S}(\vec{r}) = cr + 2m, \qquad \hat{S}(\vec{\rho}) = \frac{2}{3}c\rho + m,$$
$$\hat{V}(\vec{r}) = -\frac{4\alpha}{r}, \qquad \hat{V}(\vec{\rho}) = -\frac{3\alpha}{2\rho}. \quad (39)$$

With the help of these separated effective potentials, we can estimate the energy values of the scalar diquark and the single valence quark, which give us the three-quark core energy value at the zero order, free off the center of mass motion contribution. However, it is important to note that the effective potentials for the diquark in the Eq. (39) in fact coincide completely with the two-body potentials, derived from the original single-quark confinement scalar $S(r) = cr + m$ [see Eq. (2)] and Coulomb-like vector $V(r) = -\alpha/r$ [see Eq. (3)] mean-field potentials. This means that these effective potentials are exact for the free diquark system, but not for the bound diquark inside the baryon. In reality, the diquarks are bound with an additional valence quark and have lighter mass than free diquarks. This is why below we slightly increase the attraction in the diquark effective potential by fitting them to reproduce the quark-core energy value of the ground state nucleon, estimated by one of the methods, described in the previous section. Then we can employ the effective potentials for the solution of Eq. (29) and Eq. (33) to estimate the quark core energy values of the excited $N^*$ and $\Delta^*$ resonances by using the developed in the present section method.

### D. Self-energy diagrams contribution

The self-energy terms contain contribution both from intermediate quark ($E > 0$) and antiquark ($E < 0$) states. These diagrams describe the processes when a pion or gluon is emitted and absorbed by the same valence quark which can be excited to the intermediate quark or antiquark states.

The pion part of the self-energy term (pion cloud contribution) (see Fig. 1) is evaluated as

$$\Delta E^{(\pi)}_{\text{s.e.}} = -\frac{1}{2f_\pi^2}\sum_{a=1}^{3}\sum_{\alpha'\le\alpha_F}\int\frac{d^3\vec{p}}{(2\pi)^3 p_0}\left\{\sum_\alpha \frac{V^{a+}_{\alpha\alpha'}(\vec{p})V^{a}_{\alpha\alpha'}(\vec{p})}{E_\alpha - E_{\alpha'} + p_0} - \sum_\beta \frac{V^{a+}_{\beta\alpha'}(\vec{p})V^{a}_{\beta\alpha'}(\vec{p})}{E_\beta + E_{\alpha'} + p_0}\right\}, \quad (40)$$

with $p_0^2 = \vec{p}^2 + m_\pi^2$. The $q-q-\pi$ transition form factors are defined as:

$$V^a_{\alpha\alpha'}(\vec{p}) = \int d^3x \bar{u}_\alpha(\vec{x})\Gamma^a(\vec{x})u_{\alpha'}(\vec{x})e^{-i\vec{p}\vec{x}}, \quad (41)$$

$$V^a_{\beta\alpha'}(\vec{p}) = \int d^3x \bar{v}_\beta(\vec{x})\Gamma^a(\vec{x})u_{\alpha'}(\vec{x})e^{-i\vec{p}\vec{x}}. \quad (42)$$

The vertex function of the $\pi - q - q$ and $\pi - q - \bar{q}$ transition is

$$\Gamma^a = S(r)\gamma^5\tau^a I_c, \quad (43)$$

where $I_c$ is the color unity matrix. The expression of the $\pi - q - q$ transition form factor has been derived in Ref. [17]:

$$V^a_{\alpha\alpha'}(\vec{p}) = \sum_{l_n}(-i)^{l_n+1}\int dr r^2 [g_\alpha(r)f_{\alpha'}(r) + g_{\alpha'}(r)f_\alpha(r)]S(r)j_{l_n}(pr)Y^{m'_j-m_j}_{l_n}(\hat{p}) \times \mathcal{F}(l^\pm, l', l_n, j, j', m_j, m'_j)\langle m_l|\tau^a|m'_l\rangle\langle m_c|I_c|m'_c\rangle. \quad (44)$$

The Hermitian conjunction of the transition form factor

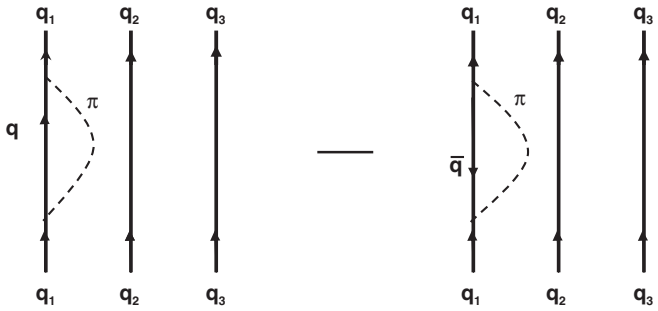


FIG. 1. Second order self-energy diagrams induced by $\pi$-meson fields

$$V^{a+}_{\alpha\alpha'}(\vec{p}) = \sum_{l_n}(i)^{l_n+1}\int drr^2[g_\alpha(r)f_{\alpha'}(r) + g_{\alpha'}(r)f_\alpha(r)]S(r)j_{l_n}(pr)Y^{(m'_j-m_j)*}_{l_n}(\hat{p}) \times\mathcal{F}(l^\pm,l',l_n,j,j',m_j,m'_j)\langle m'_t|\tau^a|m_t\rangle\langle m'_c|I_c|m_c\rangle. \quad (45)$$

After integration over the angular part in Eq. (17), the self-energy diagrams contribution to the baryon spectrum induced by pion fields is evaluated as:

$$\Delta E^{(\pi)}_{\text{s.e.}} = -\frac{1}{16\pi^3 f_\pi^2}\int\frac{dpp^2}{p_0} \times\sum_{\alpha'\le\alpha_F}\sum_{l_n}\left\{\sum_\alpha\frac{[\int drr^2G_{\alpha\alpha'}(r)S(r)j_{l_n}(pr)]^2}{E_\alpha-E_{\alpha'}+p_0} \times Q_{\text{s.e.}}(l,l',l_n,j,j') - \sum_\beta\frac{[\int drr^2G_{\beta\alpha'}(r)S(r)j_{l_n}(pr)]^2}{E_\beta+E_{\alpha'}+p_0} \times Q_{\text{s.e.}}(l,l',l_n,j,j')\right\}, \quad (46)$$

where $j_{l_n}$ is the Bessel function. The radial overlap of the single quark states with quantum numbers $\alpha=(N,l,j,m_j,m_t,m_c)$ and $\alpha'$ is defined as

$$G_{\alpha\alpha'}(r) = f_\alpha(r)g_{\alpha'}(r)+f_{\alpha'}(r)g_\alpha(r). \quad (47)$$

The angular momentum coefficients $Q$ are evaluated for all SU(2) baryons as

$$Q_{\text{s.e.}}(l,l',l_n,j,j') = 12\pi[l^\pm][l_n][j] \times\left[C^{l'0}_{l^\pm 0 l_n 0}W\left(j\frac{1}{2}l_nl';l^\pm j'\right)\right]^2 \times\sum_{m_j}\sum_{m'_J\le\alpha_f}\left[C^{j'm'_J}_{jm_jl_n(m'_J-m_j)}\right]^2, \quad (48)$$

where $C$ and $W$ are the Clebsch-Gordan and Wigner coefficients, respectively.

The gluon part of the second order self-energy diagrams (gluon cloud) contribution is estimated in a similar way as

$$\Delta E^{(g)}_{\text{s.e.}} = \frac{g_s^2}{2}\sum_a g_{\mu\nu}\sum_{\alpha'\le\alpha_F}\int\frac{d^3\vec{p}}{(2\pi)^3p}\left\{\sum_\alpha\frac{V^{a\mu+}_{\alpha\alpha'}(\vec{p})V^{a\nu}_{\alpha\alpha'}(\vec{p})}{E_\alpha-E_{\alpha'}+p} - \sum_\beta\frac{V^{a\mu+}_{\beta\alpha'}(\vec{p})V^{a\nu}_{\beta\alpha'}(\vec{p})}{E_\beta+E_{\alpha'}+p}\right\}, \quad (49)$$

where the transition form factor is evaluated with the corresponding vertex matrix

$$\Gamma^a_\mu = \gamma^\mu\frac{\lambda^a}{2}I_t \quad (50)$$

with the isospin unity matrix $I_t$.

$$V^{a\mu}_{\alpha\alpha'}(\vec{p}) = \delta_{\mu0}\int d^3x\bar{u}_\alpha(\vec{x})\frac{\lambda_a}{2}I_tu_{\alpha'}(\vec{x})\exp(-i\vec{p}\,\vec{x}) + \delta_{\mu k}\int d^3x\bar{u}_\alpha(\vec{x})\frac{\lambda_a}{2}I_t\hat{\alpha}_ku_{\alpha'}(\vec{x})\exp(-i\vec{p}\,\vec{x}). \quad (51)$$

The last expression is convenient for the estimation of the exchange diagrams.

For the self-energy diagrams we use an alternative expression of the transition form factors. Putting the quark wave functions with further integration over the radial part of the spatial coordinate one can write for the transition form factor next equation:

$$V^{a\mu}_{\alpha\alpha'}(\vec{p}) = \sum_{l_nm_n}\sum_{LL'}\sum_{m_Lm'_Lm_sm'_s}\left(\frac{[L][l_n](4\pi)}{[L']}\right)^{\frac{1}{2}}(-i)^{l_n}Y_{l_nm_n} \times(\hat{p})M^\mu_{m_sm'_s}C^{\mathrm{L}'0}_{\mathrm{L}0\mathrm{l_n}0}C^{\mathrm{jm_j}}_{\mathrm{Lm_L}\frac{1}{2}\mathrm{m_s}}C^{\mathrm{j'm'_j}}_{\mathrm{L'm'_L}\frac{1}{2}\mathrm{m'_s}}C^{\mathrm{L'm'_L}}_{\mathrm{Lm_Ll_nm_n}} \cdot\int r^2R^{\alpha\alpha'}_{\mu_{\mathrm{LL}'}}(r)j\mathrm{l_n}(pr)dr\langle m_t|I_t|m'_t\rangle\langle m_c|\frac{\lambda_a}{2}|m'_c\rangle, \quad (52)$$

where the spin transition matrices

$$M^0_{m_sm'_s} = \delta_{m_sm'_s},$$

and

$$M^k_{m_sm'_s} = \sum_{k\prime=\pm1,0}h_{kk\prime}[\delta_{k\prime1}\delta_{m_s1/2}\delta_{m'_s(-1/2)} + \delta_{k\prime(-1)}\delta_{m_s(-1/2)}\delta_{m'_s1/2}+2m_s\delta_{k\prime0}\delta_{m_sm'_s}]$$

with the only nonzero expansion coefficients $h_{1,+1}=h_{1,-1}=h_{3,0}=1$, and $h_{2,+1}=-h_{2,-1}=-i$.

The radial functions are defined as

$$R^{\alpha\alpha'}_{\mu_{LL'}}(r) = \delta_{\mu,0}\delta_{Ll}\delta_{L'l'}(g_\alpha g_{\alpha'}+f_\alpha f_{\alpha'}) + i\delta_{\mu,k}(\delta_{Ll}\delta_{L'l'^\pm}g_\alpha f_{\alpha'}-\delta_{L'l'}\delta_{Ll^\pm}g_{\alpha'}f_\alpha).$$

The corresponding Feynman diagrams are given in Fig. 2, where the contribution from intermediate quark and antiquark levels have opposite signs.

After evaluation of the transition form factors and integration over angular variables, the self-energy term induced by gluon fields can be written as a sum of color-electric (Coulomb) and color-magnetic parts (see Ref. [17]):

$$\Delta E^{(g)}_{\text{s.e.}} = \frac{g_s^2}{3\pi^2}\sum_{N'l'j'}\sum_{(\alpha,\beta)}\sum_{LL'L^*L'^*l_n}[l_n]\left(\frac{[L][L^*]}{[L'][L'^*]}\right)^{1/2} C^{L'0}_{L0l_n0}C^{L'^*0}_{L^*0l_n0}\left\{\delta_{lLL^*}\delta_{l'L'L'^*}\delta_{l_nl}\mathcal{A}^{jj'm_jm'_j}_{LL'L^*L'^*l_n}\left[\int\frac{[R_{\alpha\alpha'l_n}(p)+F_{\alpha\alpha'l_n}(p)]^2}{E_\alpha - E_{\alpha'}+p}pdp\right.\right.$$
$$\left.-\int\frac{[R_{\beta\alpha'l_n}(p)+F_{\beta\alpha'l_n}(p)]^2}{E_\beta+E_{\alpha'}+p}pdp\right] - \left[\mathcal{B}^{jj'm_jm'_j}_{LL'L^*L'^*l_n} - \mathcal{D}^{jj'm_jm'_j}_{LL'L^*L'^*l_n} + 2\mathcal{E}^{jj'm_jm'_j}_{LL'L^*L'^*l_n}\right]$$
$$\left.\times\left[\int\frac{dpp}{E_\alpha - E_{\alpha'}+p}\mathcal{H}_{\alpha\alpha'l_nLL'L^*L'^*} - \int\frac{dpp}{E_\beta+E_{\alpha'}+p}\mathcal{H}_{\beta\alpha'l_nLL'L^*L'^*}\right]\right\}, \tag{53}$$

where we define function

$$\mathcal{H}_{\alpha\alpha'l_nLL'L^*L'^*} = \mathcal{H}_{\alpha\alpha'l_nLL'L^*L'^*}(p)$$
$$= H^2_{\alpha\alpha'l_n}\delta_{lLL^*}\delta_{l'^\pm L'L'^*} + H^2_{\alpha'\alpha l_n}\delta_{l^\pm LL^*}\delta_{l'L'L'^*}$$
$$- H_{\alpha\alpha'l_n}H_{\alpha'\alpha l_n}(\delta_{lL}\delta_{l^\pm L^*}\delta_{l'^\pm L'}\delta_{l'L'^*}$$
$$+ \delta_{lL^*}\delta_{l^\pm L}\delta_{l'L'}\delta_{l'^\pm L'^*}) \tag{54}$$

and radial integrals

$$H_{\alpha\alpha'l_n} = H_{\alpha\alpha'l_n}(p) = \int dr[r^2 f_{\alpha'}(r)g_\alpha(r)j_{l_n}(pr)],$$
$$R_{\alpha\alpha'l_n} = R_{\alpha\alpha'l_n}(p) = \int dr[r^2 g_{\alpha'}(r)g_\alpha(r)j_{l_n}(pr)],$$
$$F_{\alpha\alpha'l_n} = F_{\alpha\alpha'l_n}(p) = \int dr[r^2 f_{\alpha'}(r)f_\alpha(r)j_{l_n}(pr)]. \tag{55}$$

The angular momentum coefficients $\mathcal{A}$, $\mathcal{B}$, $\mathcal{D}$, and $\mathcal{E}$ can be found from Appendix C of Ref. [17].

### E. Exchange diagrams contribution

The pion exchange contribution to the baryon energy-shift (see Fig. 3) is evaluated as:

$$\Delta E^{(\pi)}_{\text{ex}} = -\frac{1}{2f_\pi^2}\sum_{a=1}^{3}\sum_{\alpha\le\alpha_F}\sum_{\alpha'\le\alpha_F}$$
$$\times\int\frac{d^3\vec{p}}{(2\pi)^3 p_0^2}\{V^{a+}_{\alpha\alpha}(\vec{p})V^a_{\alpha'\alpha'}(\vec{p}) - V^{a+}_{\alpha\alpha'}(\vec{p})V^a_{\alpha\alpha'}(\vec{p})\}. \tag{56}$$

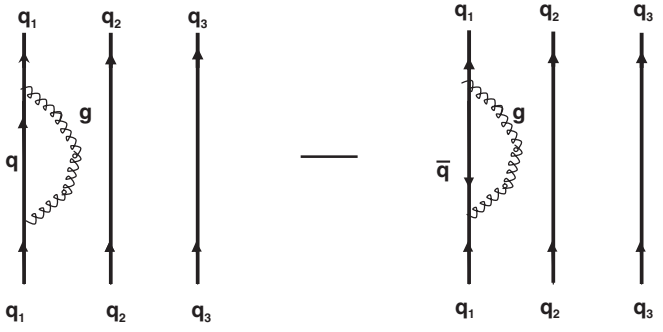


FIG. 2. Second order self-energy diagrams induced by gluon fields.

By using Wick's theorem we can write a more convenient expression for the energy shift of the SU(2) baryons from the second order pion exchange diagrams:

$$\Delta E^{(\pi)}_{\text{ex}} = -\frac{1}{16\pi^3 f_\pi^2}\int\frac{dpp^2}{p_0^2}\sum_{l_n}\Pi_{l_n}(p) \tag{57}$$

where

$$\Pi_{l_n}(p) = \left\langle\Phi_B\left|\sum_{i\ne j}\vec{\tau}(i)\vec{\tau}(j)T_{ln}(i)T_{l_n}(j)K_{l_n}(i)K^+_{l_n}(j)\right|\Phi_B\right\rangle \tag{58}$$

and the operators $\vec{\tau}$, $T_{l_n}$ and $K_{l_n}$ are summed over single quark levels $i \ne j$ of the SU(2) baryon. In the quark model, the baryon wave function $|\Phi_B\rangle$ is presented as a bound state of three valence quarks in the orbital configuration $(1S)^2(nlj)$, and it can be written down commonly as

$$|\Phi_B\rangle = |\alpha\beta\gamma\rangle(J_0T_0) = |\alpha\beta;\gamma\rangle^{TM_T(T_0)}_{JM(J_0)}$$
$$= \hat{S}[|\psi_\alpha(r_1)\psi_\beta(r_2)\psi_\gamma(r_3)\mathcal{Y}^{JM}_{J_0}(\hat{x}_1\,\hat{x}_2;\hat{x}_3)\rangle$$
$$\times|\chi^{TM_T}_{T_0}(12;3)\rangle]|\chi_c(123)\rangle,$$

where $J_0$ and $T_0$ are intermediate spin and isospin couplings of the two S-wave valence quarks, respectively. They satisfy the symmetry requirement $S_0 = T_0$. The states $\psi$ are the single particle states, labeled by a set of quantum numbers $\alpha$, $\beta$, and $\gamma$, excluding the color degree of freedom.

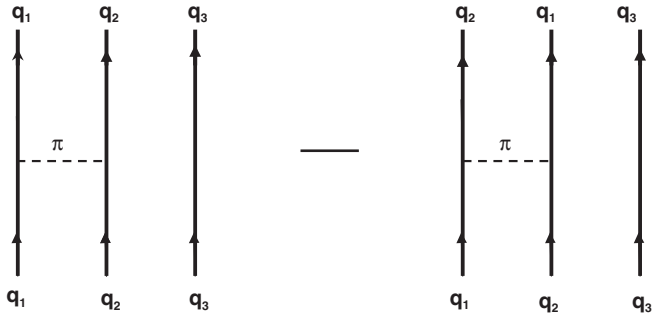


FIG. 3. Second order $\pi$-meson exchange diagrams.

The operator $T_{l_n}$ in Eq. (58) is the radial integration operator:

$$\langle\alpha|T_{l_n}|\beta\rangle = \int dr[r^2 S(r) j_{l_n}(pr) G_{\alpha\beta}(r)] \tag{59}$$

with

$$G_{\alpha\alpha'}(r) = f_\alpha(r) g_{\alpha'}(r) + f_{\alpha'}(r) g_\alpha(r), \tag{60}$$

where $\alpha = (N, l, j, m_j, m_t, m_c)$ and $\alpha'$ are two sets of the single quark quantum numbers. The matrix elements of the operator $K_{l_n}$ are given by

$$\begin{aligned}\langle\alpha|K_{l_n}|\beta\rangle = &-(4\pi[l^{\pm}(\alpha)][l_n][j(\alpha)])^{1/2} C^{l(\beta)0}_{l^{\pm}(\alpha)0 l_n 0} \\ &\times W\left(j(\alpha)\frac{1}{2} l_n, l(\beta); l^{\pm(\alpha)}, j(\beta)\right) \\ &\times C^{j(\beta)m(\beta)}_{j(\alpha)m_j(\alpha)l_n(m(\beta)-m(\alpha))},\end{aligned} \tag{61}$$

and the Hermitian conjunction

$$\langle\alpha|K^+_{l_n}|\beta\rangle = \langle\beta|K_{l_n}|\alpha\rangle,$$

where $j(\alpha)$, $l(\alpha)$, $l^{\pm}(\alpha)$, $m(\alpha)$ are the quantum numbers of the single quark state $\langle\alpha|$.

The contribution of the second-order gluon-exchange terms to the baryon spectrum (see Fig. 4) is given by

$$\begin{aligned}\Delta E^{(g)}_{\rm ex} = &-\frac{g^2}{2}\sum_{a\mu\nu}\sum_{\alpha\le\alpha_F}\sum_{\alpha'\le\alpha_F}\int\frac{d^3\vec{p}}{(2\pi)^3 p^2} \\ &\times\left\{V^{a\mu+}_{\alpha\alpha}(\vec{p})V^{a\nu}_{\alpha'\alpha'}(\vec{p}) - V^{a\mu+}_{\alpha\alpha'}(\vec{p})V^{a\nu}_{\alpha\alpha'}(\vec{p})\right\} g^{\mu\nu}.\end{aligned} \tag{62}$$

By using Wick's theorem we can write more convenient expression for this equation

$$\Delta E^{(g)}_{\rm ex} = -\frac{g^2}{\pi}\int_0^\infty dp \sum_{l_n m_n}\mathcal{Q}_{l_n m_n}(p) \tag{63}$$

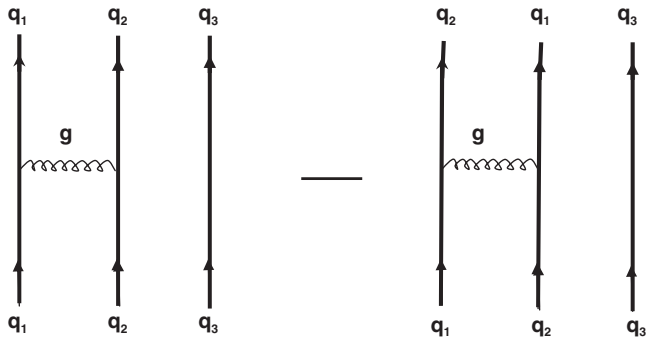


FIG. 4. Second order gluon-exchange diagrams.

with the corresponding color-electric (Coulomb) and color-magnetic parts:

$$\begin{aligned}\mathcal{Q}_{l_n m_n}(p) = &\left\langle\Phi_B\left|\sum_{i\ne j}\frac{\vec{\lambda}(i)}{2}\frac{\vec{\lambda}(j)}{2}T^{(g)}_{ln}(i)T^{(g)}_{ln}(j)\hat{F}_{l_n m_n}\right.\right. \\ &\left.\left.\times(i)\hat{F}^+_{l_n m_n}(j)\right|\Phi_B\right\rangle \\ &-\left\langle\Phi_B\left|\sum_{i\ne j}\frac{\vec{\lambda}(i)}{2}\frac{\vec{\lambda}(j)}{2}T^{(g)}_{ln}(i)T^{(g)}_{ln}(j)\hat{F}_{l_n m_n}\right.\right. \\ &\left.\left.\times(i)\hat{F}^+_{l_n m_n}(j)\hat{\vec{\alpha}}(i)\hat{\vec{\alpha}}(j)\right|\Phi_B\right\rangle.\end{aligned} \tag{64}$$

The operator $T^{(g)}_{ln}$ is the radial integration operator with the factor $j_{l_n}(pr)$. The operators $\hat{F}_{l_n m_n}(i)$ and $\hat{F}^+_{l_n m_n}(j)$ are the angular integration operator with the factors $Y_{l_n m_n}(\hat{x}_i)$ and $Y^*_{l_n m_n}(\hat{x}_j)$, respectively. All these operators are summed over single quark levels $i \ne j$ of the SU(2) baryon.

### F. Selection rules for the quantum numbers of the excited $N^*$ and $\Delta^*$ states

Now we begin to analyze the excited $N^*$ and $\Delta^*$ spectrum based on the relativistic description of one-pion and one-gluon (color magnetic part) exchange mechanisms. These exchange operators, as was found in Ref. [17], couple the upper and lower components of the two interacting valence quarks, respectively. Based on this fact we can derive the selection rules for the quantum numbers of the baryon states with the fixed orbital configuration.

Let us to fix the orbital configuration as $(1S_{1/2})^2(nlj)$, with the intermediate spin coupling $\vec{S}_0 = \vec{S}_1 + \vec{S}_2 = \overrightarrow{1/2} + \overrightarrow{1/2}$ of the two $1S$-valence quarks, where the last valence quark $(nlj)$ can be in the ground or an excited state. The upper and lower Dirac components of the last excited valence quark have orbital momenta $l$ and $l' = l \pm 1$, respectively. Our choice of the above orbital configuration is close to the limitation in the diquark-quark models [42,43], where some of the degrees of freedom are "frozen." The corresponding baryon states are different from members of the SU(6) ⊗ O(3) multiplets in the constituent quark models.

The first two selection rules come from the coupling of the three valence quarks into the SU(2) baryon state with total momentum $J$ and isospin $T$:

$$\begin{aligned}\vec{S}_0 + \vec{j} &= \vec{J}, \\ \vec{T}_0 + \overrightarrow{1/2} &= \vec{T}, \\ T_0 &= S_0,\end{aligned} \tag{65}$$

where the symmetry property of the two S-quarks coupling was used. The third rule comes from the pion exchange mechanism between the excited valence quark and the $1S$ quark. This mechanism couples the upper (lower) component of the $1S$ valence quark with the lower (upper) component of the excited $(nlj)$ valence quark. Since the upper component of the S-quark has zero orbital momentum, then for the orbital momentum of the exchanged pion we derive the equation

$$L_\pi = l' = l \pm 1. \tag{66}$$

The final selection rule is based on the assumption that the coupling of the last valence quark with quantum numbers $(nlj)$ to the $1S$ quark plus pion is the main component of the strong coupling of the excited baryon state to the $N(939) + \pi$:

$$\vec{L}_\pi + \overrightarrow{1/2} = \vec{J}. \tag{67}$$

With this assumption, Eq. (66) can be used for the identification of the baryon resonance in the $\pi N$-scattering process. Namely, when $l' = 0$ we have S-wave nucleon and delta resonances, when $l' = 1$ we have P-wave resonances, etc.

An important consequence of the obtained selection rules is that all the $N^*$ and $\Delta^*$ resonances appearing in the $\pi N$ scattering process and coupled strongly to the $\pi N$ channel are identified with the orbital configurations $(1S_{1/2})^2(nlj)$ with two valence quarks in the ground state and a single valence quark in an excited state. A baryon resonance corresponding to the orbital configuration with two valence quarks in excited states $(1S_{1/2})(nlj)_1(nlj)_2$ couples strongly to the $\pi\pi N$-channel, but not to the $\pi N$ channel.

Using the obtained selection rules it is very natural to analyze schematically the excited nucleon and delta spectrum. For the fixed orbital configurations $(1S_{1/2})^2(nlj)$ with the intermediate spin coupling of the two $S$—wave quarks $S_0 = 0$ (the so-called instanton channel), Eq. (65) allows only a single $N^*$ state with $J = j$ and no any $\Delta^*$ resonances.

Except the case, when the last valence quark is in the $P_{1/2}$ orbit, the intermediate coupling $S_0 = 1$, due to the selection rule Eq. (67) yields two resonances in the both nucleon and delta sectors with the total momentum $J = L_\pi \pm 1/2$. In this way one of the $N^*$ resonances defined by the selection rules in Eq. (65) with $J = j + 1$ or $J = j - 1$ is ruled out. When the last valence quark is in the $P_{1/2}$ orbit, i.e., has the lower S-component, the selection rules yield $L_\pi = 0$ and $J = 1/2$, and consequently, only single S-wave resonances in the both nucleon and $\Delta$ sectors are allowed.

Thus, for the fixed $(1S_{1/2})^2(nlj)$ orbital configuration with $(nlj) \neq (nP_{1/2})$ there must be a band of three $N^*$ and two $\Delta^*$ resonances. The lightest $N^*$ state corresponds to the intermediate spin coupling $S_0 = 0$ due to strong attraction in this "instanton channel." The other two $N^*$, as well as the two $\Delta^*$ resonances correspond to the spin coupling $S_0 = 1$ and must be close each to other.

In the case when the last quark is in the $P_{1/2}$ orbit, there is a band of two $N^*$ states (not close each to other) and a single $\Delta^*$ resonance appearing in the S-wave of the $\pi N$ scattering data.

## III. NUMERICAL RESULTS

### A. Condition of the calculations

In order to account for the finite size effect of the pion, we introduce a one-pion vertex regularization function in the momentum space, parametrized in the dipole form as

$$F_\pi(p^2) = \frac{\Lambda_\pi^2 - m_\pi^2}{\Lambda_\pi^2 + p^2}.$$

We fix $\Lambda_\pi = 1$ GeV in our calculations from Ref. [21] which was averaged between NN-scattering data (1–1.5 GeV) [44] and quark model studies (0.7–1 GeV) [11]. Contrary to the bag-model calculations, the above regularization is used not for the solution of the convergence problem of the quark self-energy. This was explicitly shown in Ref. [20] and [18] for the lowest valence quark states. As is known from Ref. [13], the convergence of the quark self-energy is a serious problem in the bag models and needs a a strong regularization procedure.

As was noted above, the strength $c = 0.16$ GeV$^2$ and Coulomb $\alpha = \pi/12 \approx 0.26$ parameters of the Cornell potential are fixed from the flux-tube study [36] and lattice calculations [31,32]. However, it is useful to note that the above value of the strength parameter was already probed long times ago in Ref. [21]. The only free parameter of the model, $m$ of the confining potential was chosen as m = 60 MeV to reproduce the correct axial charge of the proton $g_A = 1.26$ (and the empirical pion-nucleon coupling constant $G^2_{\pi NN}/4\pi = 14$ via the Goldberger-Treiman relation). It yields a reasonable value for the quark core RMS radius of the proton 0.52 fm (see [21]). The strong coupling constant $g_s^2 = 4\pi\alpha_s$ with the value $\alpha_s = 0.65$.

In Ref. [21] by examining the different model parameters the sensitivity of the nucleon energy on the description of the static properties of the proton has been examined. It was found that a larger value of the strength parameter $c$ of the confining potential yields a smaller value for the proton RMS radius.

Stating that the Coulomb like term of the Cornell potential $V(r) = -\alpha/r$ is actually due to the color electric component of one-gluon exchange mechanism, we need to avoid a double counting of these components in the calculations of gluon loop corrections to the baryon mass spectrum. This is why we have restricted our study to the

color-magnetic component of the one-gluon exchange forces together with one-pion loop corrections.

### B. Ground state nucleon spectrum

In Table I we give the mass values for the g.s. N(939) with and without CM correction in three different methods: the R = 0, [39], P = 0 [40], and LHO [41]. All these methods were firstly examined in Ref. [38]. As we can see from the table, they agree within 50 MeV for the ground state nucleon.

The pion loop diagrams yield positive contribution to the baryon mass-spectrum due to self-energy term. For the ground state nucleon it is 200 MeV.

For the gluon field contributions we probe two different ways. In the first case we include the contribution of all the intermediate quark and antiquark states up to convergence with $j = 25/2$. The corresponding results are given in the 3-row of Table I, they increases the nucleon mass by 109 MeV. In the second case a restriction of the intermediate states to the ground $1S$ quark state is used when estimating the self-energy (I = 0). The second approximation is based on the short-range character of one-gluon exchange forces. The corresponding energy shift for the ground state nucleon is now negative (−127 MeV). However, after including the center of mass corrections, the nucleon mass is still overestimated by about 100 MeV. In principle, we can fit the strong coupling constant $\alpha_s$ to reproduce the N(939) mass value, but first we have to check the excitation spectrum of the SU(2) flavor baryons. Thus, from the results in Table I we can conclude, that the second way, when the short-range character of one-gluon exchange forces is taken into account, is most favorable.

We note that the agreement within 50 MeV of the three R = 0 [39], P = 0 [40], and LHO [41] methods for the CM correction is reasonable. Moreover, these three methods always give corrections with systematic differences. Namely, the LHO method always yields correction larger than the $P = 0$ method, but smaller than the $R = 0$ method (see Ref. [17]). Thus, we can fix one of these methods (R = 0) and go to the excited sector.

### C. Spectrum of the SU(2) flavor baryons

In Table II we compare our numerical estimations of the excited $N^*$ and $\Delta^*$ spectrum within the developed schematic periodic table with the last experimental data from [1] and [45]. The calculations were done up-to and including F-wave baryon resonances in the frame of the developed chiral quark model. In the table we give the center of mass (CM) corrected quark core results (zero order estimation) (second column) together with the second order pion field contributions corresponding to the self energy (3rd column) and exchange diagrams (4th column).

In order to reproduce the ground state nucleon and delta quark core energy value, the parameter of the effective Coulomb-like vector potential for the diquark in Eq. (39) is slightly modified:

$$\hat{V}(\vec{r}) = -\frac{5\alpha}{r}, \tag{68}$$

while keeping other parameters of effective potentials in Eq. (39) as before. In this way the scalar diquark energy value decreases from 632 MeV to the reasonable value of 520 MeV as estimated with the help of Eq. (29). The estimated $1S_{1/2}$ single quark energy value is 420 MeV as found from the solution of Eq. (33) with the modified potentials from Eq. (39), that yields for the total quark-core energy of the ground state nucleon an estimation 940 MeV, consistent with the results of the $R = 0$ method (see Table I). At the end, by using these effective potentials we have estimated the quark-core energy values of the excited $N^*$ and $\Delta^*$ resonances on the basis of those developed in the Sec. II C method.

The 5th column of the Table II contains results for the quark core plus pion loop corrections. Next the 6th and 7th columns correspond to the contributions of the self-energy and exchange terms of the color-magnetic one-loop diagrams. The final theoretical estimations are given in the 8-column with the strong coupling constant $\alpha_s = 0.65$. As was argued above, due to the short range character of the gluon exchange forces between valence quarks, we restrict our calculations of the color-magnetic self-energy terms to the case, where the intermediate quark is the same initial and final quark.

Based on obtained selection rules first we will show the assignment of the excited baryon states presented in the data from Ref. [1] with corresponding orbital configurations. Let us fix the orbital configuration $(1S_{1/2})^2(nS_{1/2})$. In the data there are four $N^*$ with $J^\pi = 1/2^+$ ($P_{11}$ resonances) and two $N^*$ with $J^\pi = 3/2^+$ ($P_{13}$ resonances). With the above rules, we can find easily that $N^*(1440)$, $N^*(1710)$, and $N^*(1720)$ resonances belong to the orbital configuration $(1S_{1/2})^2(2S_{1/2})$ with the radially excited

TABLE I. The mass value of the g.s. nucleon in MeV with and without center of mass (CM) correction.

| | No CM | R = 0, [39] | P = 0, [40] | LHO, [41] |
|---|---|---|---|---|
| $E_Q$ | 1715 | 940 | 985 | 966 |
| $E_Q + \Delta E(\pi)$ | 1915 | 1140 | 1185 | 1166 |
| $E_Q + \Delta E(\pi + g)$ | 2024 | 1249 | 1294 | 1275 |
| $E_Q + \Delta E(\pi + g)$, I = 0 | 1788 | 1013 | 1058 | 1039 |

TABLE II. Estimations for the energy values of the $N^*$ and $\Delta^*$ resonances in MeV.

| SU(2) baryon state | $E_Q(CM\text{cor})$ | $\Delta E_\pi^{\text{s.e.}}$ | $\Delta E_\pi^{\text{ex}}$ | $E_Q+\Delta E_\pi$ | $\Delta E_g^{\text{s.e.}}$ | $\Delta E_g^{\text{ex}}$ | E(theor) | E(exp.)[1] |
|---|---|---|---|---|---|---|---|---|
| $N(939)(1/2^+)(P_{11})\ (1S)^3$ | 940 | 380 | −180 | 1140 | −95 | −32 | 1013 | 938 ÷ 939 |
| $N(1440)(1/2^+)(P_{11})\ (1S)^2(2S)$ | 1289 | 603 | −113 | 1750 | −70 | −24 | 1685 | 1430 ÷ 1470 |
| $N(1710)(1/2^+)(P_{11})\ (1S)^2(2S)$ | 1289 | 603 | −66 | 1797 | −70 | −10 | 1746 | 1650 ÷ 1750 |
| $N(1720)(3/2^+)(P_{13})\ (1S)^2(2S)$ | 1289 | 603 | 1 | 1864 | −70 | 10 | 1833 | 1700 ÷ 1760 |
| $N(1880)(1/2^+)(P_{11})\ (1S)^2(3S)$ | 1528 | 788 | −110 | 2166 | −66 | −28 | 2112 | 1840 ÷ 1940 |
| $N(2100)(1/2^+)(P_{11})\ (1S)^2(3S)$ | 1528 | 788 | −39 | 2237 | −66 | −1 | 2210 | 2000 ÷ 2200 |
| $N(1900)(3/2^+)(P_{13})\ (1S)^2(3S)$ | 1528 | 788 | −3 | 2273 | −66 | 11 | 2256 | 1900 ÷ 2000 |
| $N(1535)(1/2^-)(S_{11})\ (1S)^21P_{1/2}$ | 1186 | 501 | −119 | 1541 | −79 | −13 | 1476 | 1528 ÷ 1548 |
| $N(1650)(1/2^-)(S_{11})\ (1S)^21P_{1/2}$ | 1186 | 501 | 46 | 1706 | −79 | −49 | 1605 | 1640 ÷ 1680 |
| $N(1905)(1/2^-)(S_{11})\ (1S)^22P_{1/2}$ | 1440 | 713 | −111 | 2004 | −69 | −27 | 1946 | 1850 ÷ 1950 |
| $N(2090)(1/2^-)(S_{11})\ (1S)^22P_{1/2}$ | 1440 | 713 | 24 | 2139 | −69 | −13 | 2095 | 2100 ÷ 2260 |
| $N(1520)(3/2^-)(D_{13})\ (1S)^21P_{3/2}$ | 1165 | 515 | −126 | 1508 | −91 | −27 | 1436 | 1518 ÷ 1526 |
| $N(1700)(3/2^-)(D_{13})\ (1S)^21P_{3/2}$ | 1165 | 515 | −79 | 1555 | −91 | −9 | 1501 | 1675 ÷ 1775 |
| $N(1675)(5/2^-)(D_{15})\ (1S)^21P_{3/2}$ | 1165 | 515 | 11 | 1645 | −91 | 29 | 1629 | 1670 ÷ 1680 |
| $N(1860)(3/2^-)(D_{13})\ (1S)^22P_{3/2}$ | 1437 | 713 | −111 | 1983 | −73 | −29 | 1937 | 1810 ÷ 1890 |
| $N(2080)(3/2^-)(D_{13})\ (1S)^22P_{3/2}$ | 1437 | 713 | −31 | 2063 | −73 | −1 | 2045 | 2045 ÷ 2155 |
| $N(2200)(5/2^-)(D_{15})\ (1S)^22P_{3/2}$ | 1437 | 713 | 4 | 2098 | −73 | 20 | 2101 | 2075 ÷ 2245 |
| $N(1680)(5/2^+)(F_{15})\ (1S)^21D_{5/2}$ | 1324 | 638 | −114 | 1785 | −89 | −30 | 1729 | 1680 ÷ 1690 |
| $N(1870)(5/2^+)(F_{15})\ (1S)^21D_{5/2}$ | 1324 | 638 | −37 | 1862 | −89 | 2 | 1838 | 1840 ÷ 1960 |
| $N(1990)(7/2^+)(F_{17})\ (1S)^21D_{5/2}$ | 1324 | 638 | 12 | 1911 | −89 | 27 | 1912 | 1860 ÷ 2100 |
| $\Delta(1232)(3/2^+)(P_{33})\ (1S)^3$ | 940 | 380 | −36 | 1284 | −95 | 32 | 1221 | 1230 ÷ 1234 |
| $\Delta(1600)(3/2^+)(P_{33})\ (1S)^2(2S)$ | 1289 | 603 | −23 | 1841 | −70 | 34 | 1833 | 1535 ÷ 1695 |
| $\Delta(1750)(1/2^+)(P_{31})\ (1S)^2(2S)$ | 1289 | 603 | 1 | 1865 | −70 | 8 | 1831 | 1710 ÷ 1780 |
| $\Delta(1910)(1/2^+)(P_{31})\ (1S)^2(3S)$ | 1528 | 788 | −3 | 2273 | −66 | 23 | 2270 | 1845 ÷ 2025 |
| $\Delta(1920)(3/2^+)(P_{33})\ (1S)^2(3S)$ | 1528 | 788 | −18 | 2258 | −66 | 8 | 2240 | 1880 ÷ 2020 |
| $\Delta(1620)(1/2^-)(S_{31})\ (1S)^21P_{1/2}$ | 1186 | 501 | −24 | 1636 | −79 | 45 | 1629 | 1603 ÷ 1649 |
| $\Delta(1900)(1/2^-)(S_{31})\ (1S)^22P_{1/2}$ | 1440 | 713 | −24 | 2091 | −69 | 12 | 2072 | 1860 ÷ 1960 |
| $\Delta(1700)(3/2^-)(D_{33})\ (1S)^21P_{3/2}$ | 1165 | 515 | −18 | 1616 | −91 | 8 | 1579 | 1670 ÷ 1770 |
| $\Delta(5/2^-)(D_{35})\ (1S)^21P_{3/2}$ | 1165 | 515 | −35 | 1599 | −91 | 35 | 1589 | ... |
| $\Delta(1940)(3/2^-)(D_{33})\ (1S)^22P_{3/2}$ | 1437 | 713 | −9 | 2085 | −73 | 9 | 2077 | 1935 ÷ 2055 |
| $\Delta(1930)(5/2^-)(D_{35})\ (1S)^22P_{3/2}$ | 1437 | 713 | −22 | 2072 | −73 | 28 | 2083 | 1900 ÷ 1960 |
| $\Delta(1905)(5/2^+)(F_{35})\ (1S)^21D_{5/2}$ | 1324 | 638 | −12 | 1887 | −89 | 7 | 1868 | 1860 ÷ 1940 |
| $\Delta(1950)(7/2^+)(F_{37})\ (1S)^21D_{5/2}$ | 1324 | 638 | −27 | 1872 | −89 | 29 | 1875 | 1915 ÷ 1960 |

$2S$ valence quark state, while the other three $N^*(1880)$, $N^*(1900)$, and $N^*(2100)$ resonances correspond to the orbital configuration $(1S_{1/2})^2(3S_{1/2})$. In the $\Delta$ sector there are two resonances with $J^\pi = 3/2^+$ at 1600 MeV and 1920 MeV, and two states with $J^\pi = 1/2^+$ at 1750 MeV and 1910 MeV which belong to the orbital configuration with the radially excited valence quark in consistence with our results.

The orbital configuration $(1S_{1/2})^2(1D_{3/2})$ is not presented in the data, since it would give two $N^*$ resonances with $J^\pi = 3/2^+$ and a single $N^*$ resonance with $J^\pi = 1/2^+$.

For the orbital configurations $(1S_{1/2})^2(nP_{1/2})$ there are four nucleon and three delta resonances with $J^\pi = 1/2^-$ and they are not close each to each others. Each of the nucleon bands $n = 1$ and $n = 2$ contains two resonances, while $\Delta^*$ resonances correspond to the three bands including $n = 3$.

The orbital configuration $(1S_{1/2})^2(nP_{3/2})$ with $n = 1$ yields three $N^*$ resonances $3/2^-(1520)$, $5/2^-(1675)$, and $3/2^-(1700)$, the first of which is less than other two states in accordance with our prediction. The band with $n = 2$ yields next group of the D-wave nucleon resonances $3/2^-(1860)$, $3/2^-(2080)$ and $5/2^-(2200)$.

In the delta sector there are four D-wave resonances, however only two of them $\Delta(5/2^-)(1930)$ and $\Delta(3/2^-)(1940)$ are close each to other. Since other D-wave resonances $\Delta(3/2^-)(1700)$ and $\Delta(5/2^-)(2350)$ are far from each other, then we can predict a possible existence of new $\Delta^*(5/2^-)$ (around 1700 MeV) and $\Delta^*(3/2^-)$ (around 2350 MeV) resonances.

The F-wave $N^*$ resonances $N^*(5/2^+)(1680)$, $N^*(5/2^+)(1870)$, and $N^*(7/2^+)(1990)$ belong to the orbital configuration $(1S_{1/2})^2(nD_{5/2})$ with $n = 1$ together with delta states $\Delta^*(5/2^+)(1905)$ and $\Delta^*(7/2^+)(1950)$, while the $\Delta^*(5/2^+)(2000)$ and $\Delta^*(7/2^+)(2390)$ belong to the $n = 2$ band.

We can continue our analysis at higher energies and predict in summary seven new $N^*$ resonances with $J^\pi = 7/2^-$ (2000 MeV), $9/2^+$ (2100–2300 MeV), $11/2^+$ (2100–2300 MeV), $11/2^-$ (2500–2700 MeV), $13/2^-$ (2500–2700 MeV), $13/2^+$ (2600–2800 MeV), $15/2^+$

(2600–2800 MeV) and four $\Delta^*$ resonances with $J^\pi = 5/2^-$ (around 1700 MeV), $3/2^-$ (2350 MeV), $11/2^-$ (2750 MeV), $13/2^+$ (2950 MeV). These resonances are expected to be observed in future experiments.

It is clear now that the remaining "missing $N^*$ and $\Delta^*$ resonances" predicted by the constituent quark models must appear in the $\pi\pi N$ strong coupling sector, if they exist. As we have argued above, they will be assigned with the orbital configuration $(1S_{1/2})(nlj)_1(nlj)_2$ with two excited valence quarks and a single ground state valence quark.

Now we can analyze the numerical values within our model in comparison with the experimental data from Ref. [1]. In Figs. 5 and 6 we give the theoretical estimations and experimental data in a convenient diagrammatic way. Table II contains information about orbital configurations for each baryon resonance, as well as separate contributions from self-energy and exchange diagrams dueto pion- and color-magnetic gluon fields. As can be seen from the Table and figures, the mass spectrum of the nucleon and $\Delta$ is described reasonably well in the relativistic chiral quark model with a single free parameter of the confining potential.

For the test of the results we can check the consistence of our results with the results of the cloudy bag model [10]. The pion exchange diagrams contribute about 144 MeV to the energy difference between $N(939)$ and $\Delta(1232)$, while the gluon exchange forces yield 64 MeV for the strong coupling constant value $\alpha_s = 0.65$. The value $\alpha_s = 1.51$ increases the gluon field contribution up to 149 MeV, which is consistent with the cloudy bag model results. However, as one can see from the table, this way strongly moves down almost all the baryon states including $N(939)$ and $\Delta(1232)$.

Another very important issue is the self-energy terms. From Table II the self-energy contributions to the baryon spectra seem too large and hardly under control. However, the numbers standing in the table for the self-energy terms

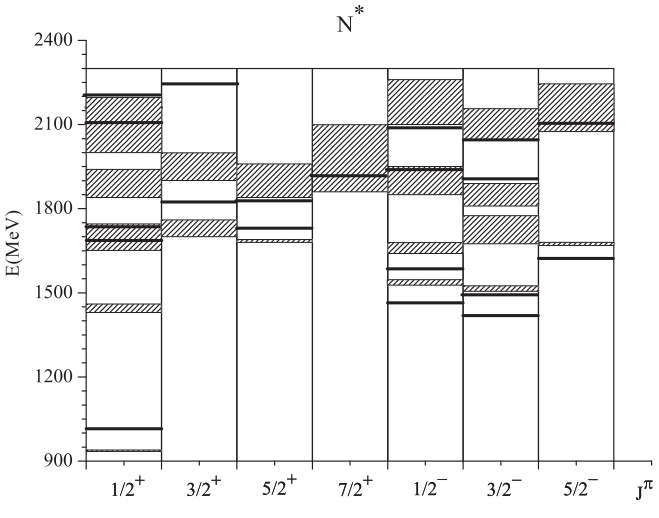


FIG. 5. Spectrum of the nucleon states. Theoretical estimations (solid lines) in comparison with experimental data (boxes) from Ref. [1].

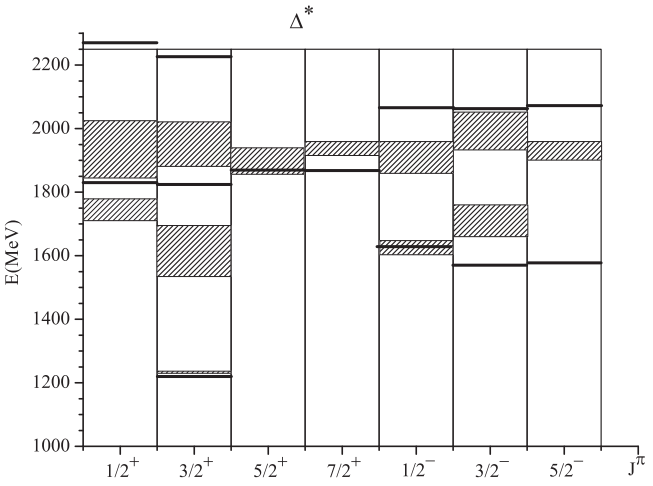


FIG. 6. Spectrum of the delta states (notations are the same as in Fig. 5).

are in fact the sums of the contributions of all intermediate quark and antiquark states to the fixed baryon spectrum. Each intermediate quark and antiquark states yields small enough contributions and can be estimated perturbatively.

The total momentum of the intermediate quark and antiquark states increases from $j = 1/2$ up to $j = 25/2$, while their radial quantum number grows up to $n = 20$ in order to reach convergent results. The total number of the self energy diagrams contributing to the fixed valence quark self-energy is $13 * 20 * 2 = 520$. A single self-energy diagram yields a negative contribution when intermediate state is a quark, and a positive contribution when intermediate state is an antiquark. These values are not so large, although their sum is a large number.

The most important contributions to the 1S (ground) state valence quark come from the intermediate 1S quark (−54 MeV) and $1P_{1/2}$ antiquark (88 MeV) states. All the intermediate states with $j = 1/2$ contribute 46 MeV, decreasing with the value of j. In practice, the intermediate states with $j > 13/2$ give no contribution to the 1S valence quark self-energy. The final summary contribution of all intermediate states to the 1S valence quark self-energy is 126.5 MeV, which yields an estimation about 380 MeV for the N(939) g.s. self-energy. In the case of the $1P_{3/2}$ valence quark, the most important contributions come from the intermediate $1P_{3/2}$ quark (−37 MeV) and $1D_{3/2}$ antiquark (100 MeV) states. In summary, the contribution of all intermediate quark and antiquark states with the total momentum $j = 3/2$ to the $1P_{3/2}$ valence quark self-energy is 75 MeV. The intermediate states with $j > 21/2$ give about 1 MeV contribution to the $1P_{3/2}$ valence quark self-energy. The total contributions of intermediate quark and antiquark states to the $1P_{3/2}$ valence quark self-energy is about 262 MeV.

As was noted in the literature [46], the convergence of the self-energy is mostly due to the strong interference of

the positive and negative energy states. Th. Gutsche and D. Robson for the first time have shown [20,21] that the g.s. baryon self energy is positive and convergent in the chiral quark potential model. In Ref. [18] we have demonstrated explicitly a convergence of the self-energy for the valence quarks in the lowest $1S$, $2S$, $1P_{1/2}$, $1P_{3/2}$ orbits induced by the pion and color-magnetic gluon fields. We have obtained convergence of the self-energy also for the excited valence quark states in the orbits $3S$, $2P_{1/2}$, $2P_{3/2}$, $1D_{5/2}$, which are included into the structure $(1S)^2(nlj)$ of the excited baryons in present study.

By summing the self energies of the three valence quarks in the excited $(1S)^2(nlj)$ nucleon and delta states, we can estimate the contribution of self-energy terms to the excitation spectrum of the SU(2) flavor baryons.

The *ab initio* lattice QCD studies in Ref. [5] have demonstrated that the dynamical and quenched QCD simulations yield very close results for the mass spectrum of the lowest negative parity resonance $\mathrm{N}(1535)(1/2-)$ in the heavy quark-mass region. However, in the light quark-mass regime the results are significantly different due the important contribution of the light sea quarks which is nothing but the self-energy contribution due to the pion field. One can find from Fig. 2 of this work that this contribution must be about 500 MeV at the physical pion mass value 140 MeV in full consistence with our numerical result for the self-energy term of this resonance presented in Table II. This comparison justifies the large and positive self-energy contribution to the baryon spectra in our studies.

The next important observation is that one needs an additional exchange mechanism for the lowering the ground state $N(939)$ and resonances $N(1440)$ (Roper), $N^*(1720)(3/2^+)$, $N^*(1880)(1/2^+)$, and $N^*(1900)(3/2^+)$. On the other hand, two of the radially excited nucleon resonances, $N^*(1710)(1/2^+)$ and $N^*(2100)(1/2^+)$ are inside the corresponding error boxes.

The close situation is in the $\Delta$ sector. The ground state $\Delta(1212)$ is well reproduced. However, the first radial excitation band is slightly overestimated [$\Delta(1600)3/2^+$ and $\Delta(1750)1/2^+$], while the second radial excitation band is overestimated strongly.

To the contrary, the first band of orbitally excited $N^*$ resonances with a negative parity are mostly underestimated. The second band is inside or close to the experimental box. The situation in the $\Delta^*$ sector is close. The orbitally excited $\Delta^*$ states corresponding to the lowest radial quanta $n = 1$ are slightly underestimated or inside the experimental box, while negative parity $\Delta$ states corresponding to the radial quantum number $\mathrm{n} = 2$ are mostly overestimated.

The orbitally excited nucleon and delta resonances with the positive parity are reproduced quite well in the developed model.

It is relevant to compare the obtained estimations for the excited $\mathrm{N}^*$ and $\Delta^*$ spectrum with the results of the relativized constituent quark model [8]. A comparison of the results presented in the Figs. 5 and 6 with the results presented in Fig. 9 and Fig. 10 of the above-mentioned work indicates that the two methods describe the excited baryon spectrum approximately at the same level. However, the present model does not have any fitting parameters, and, additionally, unlike CQM, it does not predict many missing nonobserved resonances.

The analysis shows that one needs an additional exchange mechanism between valence quarks to reproduce the whole SU(2) baryon spectrum. The new exchange forces must depend on the spin and flavor of valence quarks as well as on the quantum numbers of the baryon state. Of course, a large part of the interaction comes from two-pion exchange mechanism.

A serious question is whether the two-pion loop corrections to the baryon energy spectrum are small enough and under control? Consistent complete estimations can be obtained only when including all fourth order (two loop) corrections induced by the pion field to the baryon mass spectrum. This study requires much more effort than for the second order corrections in the present manuscript. They are a subject of very extensive studies in the future.

In order to check whether the next fourth order corrections due to the pion field are reasonably small and under control, we have done test calculations for the correlated two-pion loop corrections to the excited baryon resonances spectrum. Namely, we estimated the second order corrections corresponding to the self-energy and exchange diagrams induced by the scalar sigma- and vector rho-meson fields. The results indicate that these corrections are under control. For example, the both self energy and exchange diagrams due to the sigma meson fields yield negative contributions to the baryon energies (up to $-50$ MeV and $-30$ MeV, for the self-energy and exchange terms, respectively). The corresponding contributions from the self-energy diagrams due to rho-meson fields are positive (up to 50 MeV), while exchange terms are negative for the nucleon states (of order $-10$ MeV) and positive for the delta states (of the same order).

These test calculations present only a part of the complete fourth order corrections induced by the pion field, which must be derived from Eq. (14). This is why we did not include the results of these test calculations to the final results.

The numerical results given in Tables I and II, and Figs. 5 and 6 present the final estimations for the baryon energy spectrum at the second order level.

## IV. CONCLUSIONS

In summary, we have derived selection rules for the excited baryon state, assuming that it's orbital configuration is of the form $(1S)^2(nlj)$ with two valence quarks in the ground state and a single excited quark. These selection rules were derived on the basis of the one-pion exchange

mechanism between valence quarks in the frame of the relativistic chiral quark model. An important consequence of the obtained selection rules is that all the $N^*$ and $\Delta^*$ resonances appearing in the $\pi N$ scattering process and strongly coupled to the $\pi N$ channel are identified with the orbital configurations $(1S_{1/2})^2(nlj)$. Baryon resonances corresponding to the orbital configuration with two valence quarks in excited states couple strongly to the $\pi\pi N$-channel, but not to the $\pi N$ channel.

Based on obtained selection rules, we have constructed a schematic periodic table and calculated the energy spectrum of the excited $N^*$ and $\Delta^*$ baryons within the field-theoretical framework including one-pion and one-gluon loop corrections. The zero-order energy values of the SU(2) flavor baryons are estimated including the center of mass corrections in a new method, based on the separation of the three-quark core Hamiltonian into three parts, corresponding to the Jacobi coordinates. The obtained numerical estimations for the energy positions of baryon resonances (up to and including F-wave) yield an overall good description of the experimental data. However, nucleon ground state and most of the radially excited nucleon resonances (including Roper) are overestimated. To the contrary, the first band of the orbitally excited $N^*$ resonances with a negative parity are underestimated, while the second band is close to the experimental boxes. The positive parity nucleon resonances with $J = 5/2+$ and $7/2+$ are within or close to the experimental boxes. In the $\Delta$ sector we have a similar situation, however, the second excitation band ($n = 2$) of the orbitally excited $\Delta$ states with a negative parity are mostly overestimated. At the same time, the ground state $\Delta(1232)$ is well reproduced.

The important observation is that one needs an additional exchange mechanism for the lowering both the ground state $N(939)$ and the radially excited $N^*$ and $\Delta^*$ resonances, including the Roper resonance $N(1440)$. Of course, the two-pion exchange forces are expected to contribute essentially to the excited baryon spectrum.

A comparison of the obtained results with the results of the relativized constituent quark model indicates that they describe the excited baryon spectrum approximately at the same level. This level of description in our model was achieved without any fitting parameters. Moreover, unlike CQM, our model does not yield many nonobserved resonances at the lower excitation spectrum. The only $\Delta(5/2^-)$ resonance is expected to be observed at energy scale around 1600–1800 MeV.

At higher energies, where the experimental data are poor, we can extend our model schematically and predict the existence of seven new $N^*$ and four $\Delta^*$ states with larger spin values. Of course, the number of "missing resonances" in our model is strongly suppressed due to restriction of the configuration space to the orbits $(1S_{1/2})^2(nlj)$. However, as we have shown above, at lower energies this construction works reasonably well.

## ACKNOWLEDGMENTS

One of the authors (E. M. T.) thanks Th. Gutsche for his valuable advices and discussions, A. Faessler and B. S. Yuldashev for their support and interest, A. Rakhimov, U. Yakhshiev, H. C. Kim, V. Petrov, D. Baye for very useful discussions, and K. Shimizu for the help in the calculations of the center of mass corrections for the ground state Nucleon and Delta baryons. His work was supported in part by the DAAD (Germany) Research Fellowship Programmes. He acknowledges Institute of Theoretical Physics, University of Tuebingen and the Institute fuer Kernphysik, Forschungszentrum Juelich for the kind hospitalities during his research stays.

[1] E. Klempt and J. M. Richard, Rev. Mod. Phys. **82**, 1095 (2010).
[2] Z. Fodor and C. Hoelbling, Rev. Mod. Phys. **84**, 449 (2012).
[3] M. S. Mahbub, W. Kamleh, D. B. Leinweber, A. O. Cais, and A. G.Williams, Phys. Lett. B **693**, 351 (2010).
[4] R. G. Edwards, J. J. Dudek, D. G. Richards, and S. J. Wallace, Phys. Rev. D **84**, 074508 (2011).
[5] M. S. Mahbub, W. Kamleh, D. B. Leinweber, P. J. Moran, and A. G. Williams, Phys. Rev. D **87**, 011501(R) (2013).
[6] L. Y. Glozman, W. Plessas, K. Varga, and R. F. Wagenbrunn, Phys. Rev. D **58**, 094030 (1998).
[7] S. Capstick and N. Isgur, Phys. Rev. D **34**, 2809 (1986).
[8] S. Capstick and W. Roberts, Prog. Part. Nucl. Phys. **V45**, S241 (2000).
[9] U. Löring, K. Kretzschmar, B. C. Metsch, and H. R. Petry, Eur. Phys. J. A **10**, 309 (2001); U. Löring, B. C. Metsch, and H. R. Petry, Eur. Phys. J. A **10**, 395 (2001); **10**, 447 (2001); B. Metsch, U. Löring, D. Merten, and H. Petry, Eur. Phys. J. A **18**, 189 (2003).
[10] S. Theberge, A. W. Thomas, and G. A. Miller, Phys. Rev. D **22**, 2838 (1980).
[11] A. W. Thomas, S. Theberge, and G. A. Miller, Phys. Rev. D **24**, 216 (1981).
[12] A. W. Thomas, Prog. Part. Nucl. Phys. **61**, 219 (2008); F. Myhrer and A. W. Thomas, Phys. Lett. B **663**, 302 (2008).
[13] K. Saito, Prog. Theor. Phys. **V71**, 775 (1984).
[14] S. Nagai, T. Miyatsu, and K. Saito, Phys. Lett. B **666**, 239 (2008).
[15] M. Wakamatsu, Eur. Phys. J. A **44**, 297 (2010).

[16] E. M. Tursunov, J. Phys. G **31**, 617 (2005).
[17] E. M. Tursunov, J. Phys. G **36**, 095006 (2009).
[18] E. M. Tursunov, J. Phys. G **37**, 105013 (2010).
[19] E. Oset, R. Tegen, and W. Weise, Nucl. Phys. **A426**, 456 (1984).
[20] Th. Gutsche and D. Robson, Phys. Lett. B **229**, 333 (1989).
[21] Th. Gutsche, Ph.D thesis, Florida State University, 1987.
[22] V. E. Lyubovitskij, Th. Gutsche, A. Faessler, and R. Vinh Mau, Phys. Lett. B **520**, 204 (2001).
[23] V. E. Lyubovitskij, Th. Gutsche, and A. Faessler, Phys. Rev. C **64**, 065203 (2001).
[24] Th. Gutsche, V. E. Lyubovitskij, and A. Faessler, Prog. Part. Nucl. Phys., **50**, 235 (2003).
[25] K. Pumsa-Ard, V. E. Lyubovitskij, Th. Gutsche, A. Faessler, and S. Cheedket, Phys. Rev. C **68**, 015205 (2003).
[26] A. Faessler, Th. Gutsche, and V. E. Lyubovitskij, Prog. Part. Nucl. Phys., **55**, 1 (2005).
[27] T. Inoue, V. E. Lyubovitskij, Th. Gutsche, and A. Faessler, Int. J. Mod. Phys. E **15**, 121 (2006).
[28] V. E. Lyubovitskij, Th. Gutsche, A. Faessler, and E. G. Drukarev, Phys. Rev. D **63**, 054026 (2001).
[29] T. Inoue, V. E. Lyubovitskij, Th. Gutsche, and A. Faessler, Phys. Rev. C **69**, 035207 (2004).
[30] V. E. Lyubovitskij, P. Wang, Th. Gutsche, and A. Faessler, Phys. Rev. C **66**, 055204 (2002).
[31] T. Kawanai and S. Sasaki, Prog. Part. Nucl. Phys. **67**, 130 (2012); Phys. Rev. D **85**, 091503(R) (2012).
[32] J. Greensite and S. Olejnik, Phys. Rev. D **67**, 094503 (2003).
[33] M. Gell-Mann and M. Levy, Nuovo Cimento **16**, 705 (1960).
[34] W. Weise, in *Quarks and Nuclei*, edited by W. Weise, International Review of Nuclear Physics Vol. 1 (World Scientific, Singapore, 1984), p. 58.
[35] S. Coleman, in *Hadrons and Their Interactions* (Academic Press, New York, 1968).
[36] M. Lüscher, Nucl. Phys. **B180**, 317 (1981).
[37] A. I. Fetter and J. D. Waleska, *Quantum Theory of Many Particle Systems* (McGraw-Hill, New York, 1971).
[38] Y. B. Dong, K. Shimizu, A. Faessler, and A. J. Buchmann, Phys. Rev. C **60**, 035203 (1999).
[39] D. H. Lu, A. W. Thomas, and A. G. Williams, Phys. Rev. C **57**, 2628 (1998).
[40] R. Tegen, R. Brockmann, and W. Weise, Z. Phys. A **307**, 339 (1982).
[41] L. Wilets, *Non-Topological Solitons* (World Scientific, Singapore, 1989).
[42] M. Anselmino, E. Predazzi, S. Ekelin, S. Fredriksson, and D. B. Lichtenberg, Rev. Mod. Phys. **65**, 1199 (1993).
[43] E. Santopinto, Phys. Rev. C **72**, 022201 (2005).
[44] K. Holinde, Phys. Rep. **68**, 121 (1981).
[45] A. V. Anisovich, E. Klempt, V. A. Nikonov, A. V. Sarantsev, and U. Thoma, Eur. Phys. J. A **47**, 27 (2011).
[46] E. Oset, Nucl. Phys. **A411**, 357 (1983).